

Preparation of Promoted Ni_{0.1}Co_{0.9}Fe₂O₄ Ferrite Nanoparticles and Investigation of Its Catalytic Activity on Decomposition of H₂O₂ and Optical Characterization of Pure Ni_{0.1}Co_{0.9}Fe₂O₄

Mir Hasan Hosseini^{1,2*}, Meysam Sadeghi¹

¹ *Department of Chemistry, Imam Hossein University, Tehran, Iran*

² *Nano Center Research, Imam Hossein University, Tehran, Iran*

Received: 17 October 2012; Accepted: 22 December 2012

ABSTRACT

Pure and ZnO-doped Ni_{0.1}Co_{0.9}Fe₂O₄ catalyst were prepared by co-precipitation method and thermal decomposition in air calcinated at 400-700°C and that treated with different amounts of zinc nitrate (0.46-2.25 w% ZnO). X-ray powder diffractometry, scanning electron microscopy (SEM) and BET analysis of nitrogen adsorption isotherms investigated the crystalline bulk structure and the surface area of pure and doped samples, respectively. The hydrogen peroxide decomposition activity was determined by oxygen gasometry of the reaction kinetics at 20-40°C. The results revealed that the treatment of Ni_{0.1}Co_{0.9}Fe₂O₄ with ZnO at 400-700°C brought about a significant increase in the specific surface area and catalytic activity of Ni_{0.1}Co_{0.9}Fe₂O₄ on decomposition of hydrogen peroxide. However, the catalytic activity of H₂O₂ decomposition on Ni_{0.1}Co_{0.9}Fe₂O₄ calcined at different temperatures was found to show a considerable increase by doping with ZnO. They were discussed with UV/VIS spectroscopy which the energy band gap of the synthesized Ni_{0.1}Co_{0.9}Fe₂O₄ nano structure was calculated to be ~5 eV.

Keyword: Nickel cobalt ferrite; Nanoparticles; Catalytic activity; Decomposition of hydrogen peroxide; Calcination temperature; Promoter, Optical characterization

1. INTRODUCTION

In recent years, hydrogen peroxide has been used as an oxidant for several types of low temperature liquid-based fuel cells, including direct methanol-hydrogen peroxide fuel cell, direct borohydride-hydrogen peroxide fuel cell; hydrazine-hydrogen

peroxide fuel cell, biofuel-hydrogen peroxide fuel cell, and metal-hydrogen peroxide semi fuel cell [1]. The catalytic activity and selectivity of a catalyst are influenced by several factors such as the preparation procedure [2, 3], nature of support

(*) Corresponding Author - e-mail: hoseiny.inorganic@gmail.com

[4, 5], active phase precursor employed [6-8] and the doping with foreign ions. The surface characteristics of a large variety of solids can be influenced by the doping process. Other properties such as thermal stability and oxidation state of solid catalysts could also be modified by concentrations of certain foreign oxides [9]. NiFe_2O_4 , (NiO , Fe_2O_3) and CoFe_2O_4 (CoO , Fe_2O_3) powder is by doping with a small important transition metal oxide because of its applications in various fields of research and industry including pigments, gas sensor, magnetic materials, catalysts, anode materials for rechargeable Li-batteries, electronic devices, electrochemical systems, high-temperature solar selective absorbers and catalytic decomposition of hydrogen peroxide [10, 11].

Cobalt mixed oxides is commonly employed in various industries. Various grades of blue colouration in glass and ceramic technology are currently obtained by treating with different amounts of pure cobalt mixed with other oxides [12]. The surface characteristics of a large variety of solids can be influenced by the doping process [13]. Other properties such as thermal stability and oxidation state of solid catalysts could also be modified by doping with small concentrations of certain foreign oxides. Doping with various foreign oxides [14, 15] can change the thermal stability of mixed cobaltic oxides. The observed changes in the thermal stability of $\text{Ni}_{0.1}\text{Co}_{0.9}\text{Fe}_2\text{O}_4$ due to doping with small amounts of foreign oxides have been attributed to the dissolution of some of doped oxides added in the lattice oxide solid, forming solid solutions with subsequent changes in the oxidation state of cobalt ions in mixed cobaltic oxides solid. The increase in the oxidation state of cobalt ions results from conversion of some of Co^{2+} into Co^{3+} ions, while decrease in the oxidation state takes place through the transformation of some trivalent cobalt ions into Co^{2+} ions. The increase of oxidation state of cobalt ion due to doping induces an increase in the thermal stability of the treated cobaltic oxide solid and vice versa [16]. The induced changes in the oxidation state of cobalt ions in Co_3O_4 due to doping is expected to be accompanied by corresponding changes in its

surface area and its catalytic activity. The present study reports on the effect of ZnO addition on the specific surface area and catalytic activity of mixed cobaltic oxide catalyst calcined at different temperatures. The calcination products were characterized for the crystalline bulk structure by X-ray powder diffractometry and the specific surface area by nitrogen sorption.

2. EXPERIMENTAL

2.1. Materials

Nanocrystalline $\text{Ni}_{0.1}\text{Co}_{0.9}\text{Fe}_2\text{O}_4$ particles with compositions have been synthesized by a chemical Co-precipitation method (method 1). The starting materials used were AR grade $\text{NiCl}_2 \cdot 6\text{H}_2\text{O}$ (Fluka), $\text{CoCl}_2 \cdot 6\text{H}_2\text{O}$ (Fluka) and FeCl_3 (BDH). For synthesis, equimolar solutions of $\text{NiCl}_2 \cdot 6\text{H}_2\text{O}$, $\text{CoCl}_2 \cdot 6\text{H}_2\text{O}$ and FeCl_3 were mixed in their stoichiometric ratio and homogenized at 60°C . To this, 25% ammonia solution was added dropwise with constant stirring. The pH of the solution was maintained at 8.5. The mixture was then heated at 80°C for about 1 h. To prevent agglomeration a surfactant coating of oleic acid was made to the individual particles in the beginning itself.

The precipitated particles were then washed several times with double distilled water to remove the salt residues and other impurities. It was further dried at 80°C and was calcined in 300°C to obtain the fine powder. In method 2, Pure and doped cobalt mixed oxide specimens were prepared by thermal decomposition of pure basic $\text{CoCl}_2 \cdot 6\text{H}_2\text{O}$ (Fluka) treated with different concentrations of zinc nitrate (BDH). The doped catalyst samples with different amounts of zinc nitrate dissolved in the least amount of distilled water making pastes. The pastes were dried at 100°C to constant weights, and then heated in air at 400, 500, 600 and 700°C for 6 h. The concentrations of dopant were 0.46, 0.91 and 2.25 wt% ZnO.

2.2. Techniques

A Scifert3003TT diffractometer was used to perform X-ray powder diffractometry of pure and

variously doped samples preheated in air at 400-700°C. The patterns were run with Fe-filtered cobalt radiation ($k = 1.7889 \text{ \AA}^\circ$) at 30 kV and 10 mA with a scanning speed in 2h of 2° min^{-1} . An infrared transmission spectrum was determined for each solid using via Beckman spectrometer IR 4250. The IR spectra were determined from 4000 to 200 cm^{-1} but the portions between 1300 and 400 cm^{-1} were considered in this investigation. The sample disks were placed in the holder of double-grating IR spectrometer. The specific surface area (m^2/g) was determined via BET analysis of N_2 adsorption isotherms measured on the tested catalysts at liquid nitrogen temperature, by using a conventional volumetric apparatus. Prior to exposure to the adsorptive molecules, the investigated catalysts were out-gassed at 200°C and 10-5 Torr for 2 h. The decomposition of hydrogen peroxide was studied with catalyst $\text{Ni}_{0.1}\text{Co}_{0.9}\text{Fe}_2\text{O}_4$ with concentration of 5% at room temperature. Catalytic measurements were carried out by using the gasometric technique about 0.1g of the catalyst was added to a known amount of hydrogen peroxide (10 mL, 5%v/v) taken in a closed reaction vessel and the contents were stirred at 313 K. The volume of oxygen evolved was measured at regular time intervals. The catalytic activity calculated from equation $a = k/(t.m)$ (1) where a is the activity, k is a constant (mass of 5% hydrogen peroxide for production 100 mL O_2), t is reaction time for hydrogen peroxide decomposition and m is mass of catalyst.

3. RESULTS AND DISCUSSION

3.1. XRD investigation

X-ray diffractograms of pure $\text{Ni}_{0.1}\text{Co}_{0.9}\text{Fe}_2\text{O}_4$ and those treated with different amounts of zinc nitrate and precalcined at 400, 500, 600 and 700°C were measured. The diffraction patterns of pure and doped solids calcined at 400-700°C showed that these solids consisted mainly of a well-crystallized $\text{Ni}_{0.1}\text{Co}_{0.9}\text{Fe}_2\text{O}_4$ phase. However, the increase in the precalcination temperature of pure and doped solids from 400 to 700°C resulted in a significant

increase in the relative intensity of the lines of mixed oxide phase. XRD patterns of pure solid samples calcined at 400-700°C are shown in Figure 1. It is seen that $\text{Ni}_{0.1}\text{Co}_{0.9}\text{Fe}_2\text{O}_4$ peaks on pure sample calcined at 700°C are sharper than that on pure specimen calcined at 500°C, indicating a higher degree of crystallinity of $\text{Ni}_{0.1}\text{Co}_{0.9}\text{Fe}_2\text{O}_4$ on the former's solid sample. Figure 2 depicts the X-ray diffractograms of the pure and doped solids calcined at 700°C. It is seen from Figure 2 that doping of $\text{Ni}_{0.1}\text{Co}_{0.9}\text{Fe}_2\text{O}_4$ with ZnO followed by heating at 700°C did not lead to the formation of new crystalline compounds and most of the dopant ions added dissolved in $\text{Ni}_{0.1}\text{Co}_{0.9}\text{Fe}_2\text{O}_4$ lattice forming solid solution. It can be noted clearly that the ferrite, according to the standard XRD patterns of the spinel ferrite in all cases, is phase-pure spinel structure. The average size of crystallite was calculated using software Originpro75 through diffraction which gives Scherer's formula as shown below:

$$D = 0.89\lambda / \beta \cos\theta$$

where D , λ , β and θ are crystallite size, X-ray wave length, broadening of the diffraction peak and diffraction angle respectively. The mean size of crystallite of the pure and promoted ferrite particles calcined at 400°C is 45 nm and 27 nm respectively.

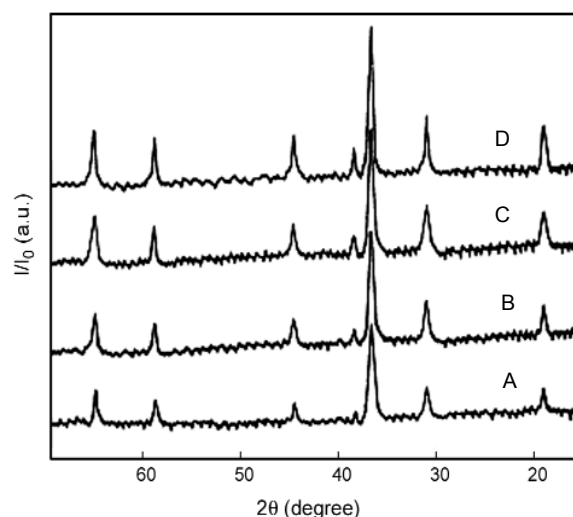


Figure 1: XRD pattern of pure $\text{Ni}_{0.1}\text{Co}_{0.9}\text{Fe}_2\text{O}_4$ nanoparticles at different calcination temperatures (A: 400°C, B: 500°C, C: 600°C and D: 700°C)

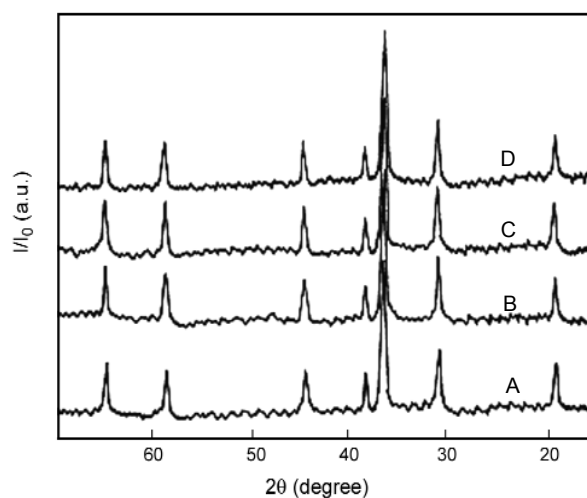


Figure 2: XRD pattern of doped $Ni_{0.1}Co_{0.9}Fe_2O_4$ calcined at $700^\circ C$ (A: pure, B: +0.46 wt% ZnO, C: +0.91 wt% ZnO and D: +2.25 wt% ZnO).

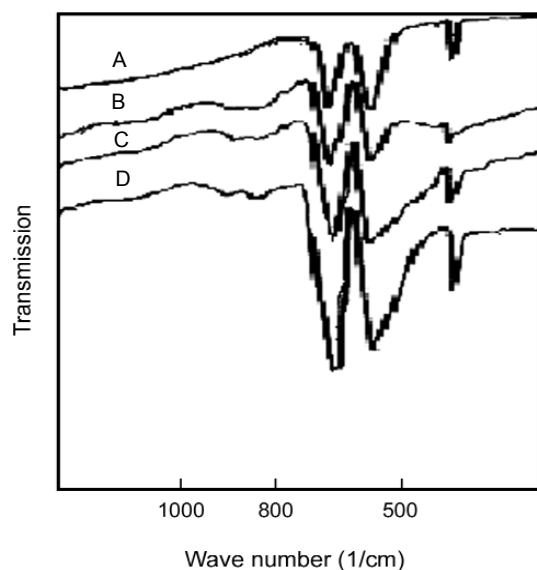


Figure 3: IR spectrum of pure and doped cobalt mixed oxide (A: pure, B: +0.46 wt% ZnO, C: +0.91 wt% ZnO and D: +2.25 wt% ZnO).

3.2. IR investigation

The IR transmission spectra were measured for pure and doped solids calcined at 400, 500, 600 and $700^\circ C$. The obtained transmission spectra for pure and ZnO-doped samples calcined at different temperatures were similar to each other. Figure 3 depicts IR spectra of pure and doped catalyst

samples calcined at $700^\circ C$. These spectra consisted of seven bands at 670, 660, 645, 588, 577, 420 and 390 cm^{-1} . These bands correspond to cobalt mixed oxide structure in the form of $Ni_{0.1}Co_{0.9}Fe_2O_4$.

3.3. Morphology investigation

Analyzing the morphology aspect of the nanoparticles by studying the SEM (micrographs) indicates that the synthesized nanoparticles are quasi-spherical and the size is less than 100 nm. That means the synthesized catalysts have nano dimension. The information obtained from XRD also confirms the above findings. The results obtained from the calculation of average size of nano-particles by the aid of SEM images and analytical Clemex image software is as followed:

The mean sizes of pure and promoted samples prepared by co-precipitation method are 50 nm and 31 nm respectively (Figure 4). It should be mentioned that the determination of nanoparticles size by aid of SEM is related to morphology of the particles that means the reported size of the nanoparticles verified by XRD and SEM techniques are related to uniform distribution of particle size. SEM images demonstrated the fact that the morphology of majority of nanoparticle is quasi-spherical.

3.4. Decomposition of H_2O_2 based on BET surface areas analysis

The specific surface areas (SBET, m^2/g) of pure and doped cobaltic mixed oxide solids calcined at $400\text{-}700^\circ C$ were determined from nitrogen adsorption isotherms. The data of SBET and hydrogen peroxide decomposition of pure and doped solids are given in Table 1 and Figures 5, 6. It is seen from Table 1 and Figures 5, 6 that ZnO doping (0.46-2.25 wt%) of cobaltic mixed oxide followed by calcination at $400\text{-}700^\circ C$ resulted in a progressive increase in its BET surface area and catalytic activity of nanoparticles on decomposition of hydrogen peroxide. The maximum increase in SBET of cobaltic mixed oxide due to doping with 2.25 wt% ZnO reached 39%, 62%, 60% and 79% for the samples precalcined at 400, 500, 600 and $700^\circ C$, respectively. However, the increase in

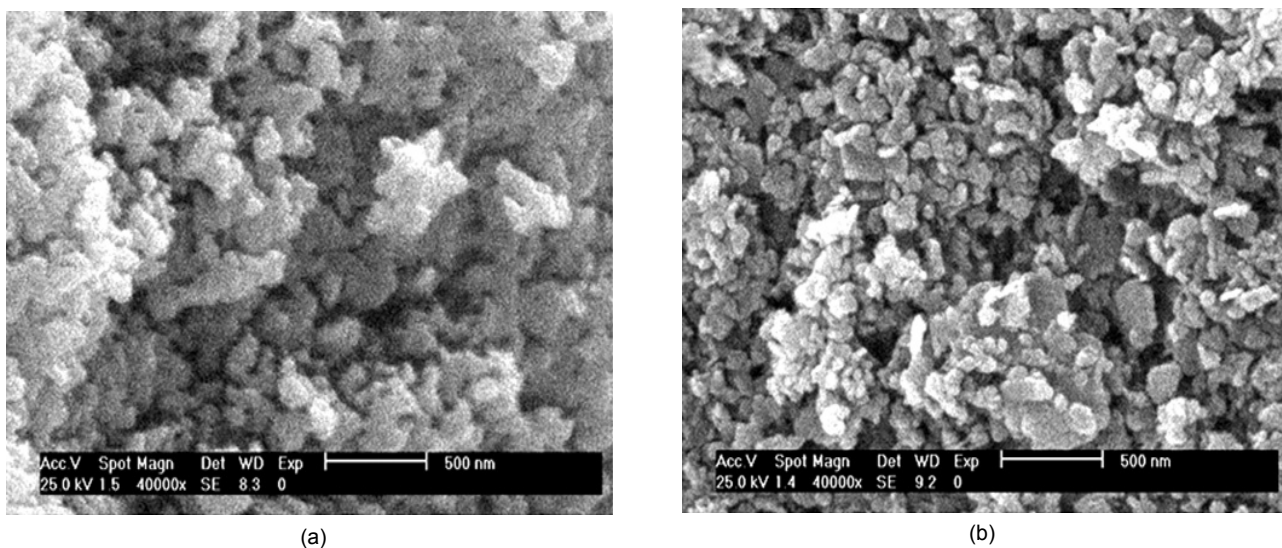


Figure 4: SEM micrographs of pure (A) and 2.25 wt% ZnO promoted (B) Nickel cobalt ferrite nanoparticles (obtained by co-precipitation method).

Table 1: BET surface areas of pure and doped solids precalcined at different temperatures.

Dopant concentration (wt% ZnO)	Calcination temp. (°C)	SBET (m ² /g)	Time of H ₂ O ₂ decomposition(s)	Calcination Temp. (°C)	SBET (m ² /g)	Time of H ₂ O ₂ decomposition (s)
0.00	400	68	135	600	40	185
0.46	400	75	105	600	52	163
0.91	400	83	90	600	65	142
2.25	400	96	35	600	70	105
0.00	500	43	170	700	34	220
0.46	500	55	153	700	42	195
0.91	500	67	120	700	50	170
2.25	500	79	85	700	62	130

calcination temperatures of pure and doped catalysts from 400 to 700°C induced a decrease in their surface areas and hydrogen peroxide decomposition activity. This decrease was more pronounced for pure and doped solids precalcined at 700°C.

The observed increase in the specific surface area and catalytic activity of cobalt mixed oxide due to doping with ZnO could be attributed to the creation of new pores resulting from the liberation of gaseous nitrogen oxides in the course of thermal dissociation of zinc nitrate. The induced decrease in

the SBET and catalytic activity of pure and doped solids due to the thermal treatment by heating at 400-700°C might be attributed to grain growth of the particles of cobaltic mixed oxide.

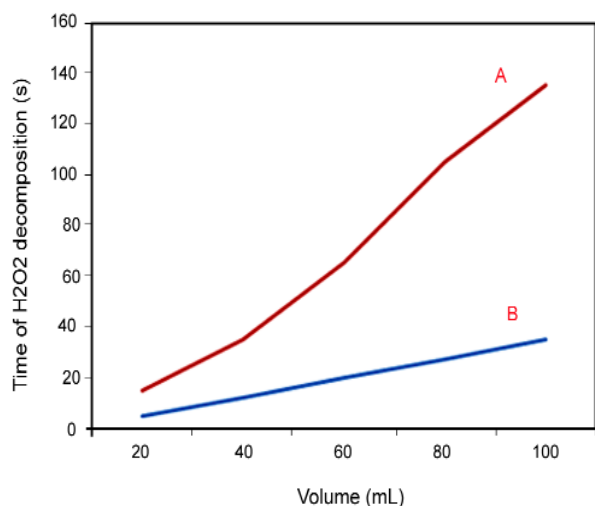


Figure 5: Plot of evolved oxygen volume as a function of time (A: pure, B: 2.25%wt calcinated at 400°C).

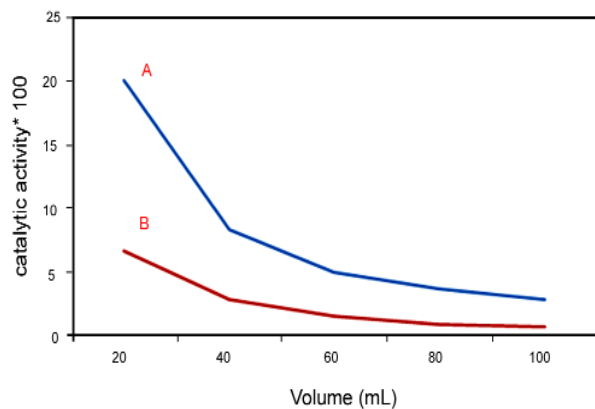


Figure 6: Catalytic activity of Ni_{0.1}Co_{0.9}Fe₂O₄ as a function of released oxygen volume (A: 2.25%wt calcinated at 400°C, B: pure).

3.5. Energy band gap calculation of Ni_{0.1}Co_{0.9}Fe₂O₄ nanocrystals

The optical properties of the nanoparticles were calculated with the help of optical absorption and percentage transmission data. The absorption and transmission spectra of the Ni_{0.1}Co_{0.9}Fe₂O₄ nanocrystals are shown in Figure 7. The absorption

coefficient α of the Ni_{0.1}Co_{0.9}Fe₂O₄ nanoparticles has been determined from the absorption and transmission data by using the fundamental relationships:

$$I=I_0e^{\alpha t} \tag{2}$$

$$A= \log (I_0 / I) \tag{3}$$

and

$$\alpha= 2.303(A / t) \tag{4}$$

Where A is the absorption and t is the thickness of the Ni_{0.1}Co_{0.9}Fe₂O₄ sample. To estimate the optical absorption edge for these nanoparticles, $(\alpha hv)^{1/n}$ was plotted as a function of the photon energy hv for different n values (n=1/2, 3/2, 2, 3) (Tauc plots) [17].

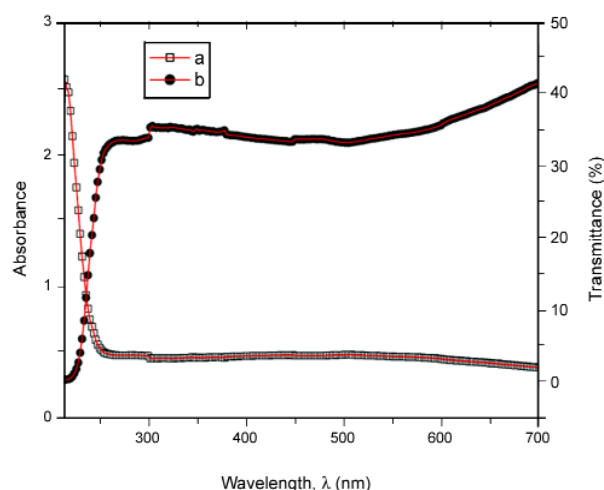


Figure 7: Plot of (a) absorption and (b) transmittance T (%) as a function of wavelength λ (nm) for Ni_{0.1}Co_{0.9}Fe₂O₄ nanostructures.

The best linear fit is obtained in the case of n=1/2, which indicates a direct allowed optical transition in Ni_{0.1}Co_{0.9}Fe₂O₄ nanoparticles. The Tauc plot is presented in Figure 8. The straight line fit to the $(\alpha hv)^2$ vs. hv plot is obtained by using a linear regression software with only very small standard deviation. The intercept of the line at $\alpha=0$ gives the value of the optical absorption edge. From

Figure 8, the value of the energy band gap is found to be approx. 5.0 eV.

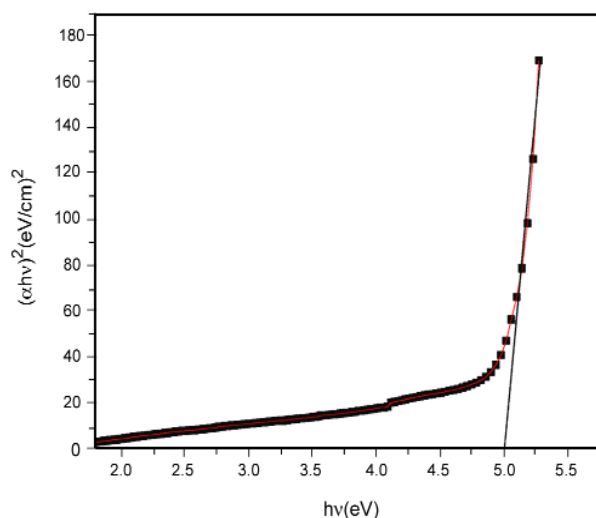


Figure 8: Plot of $(\alpha hv)^2$ as a function of photon energy (eV) for $Ni_{0.1}Co_{0.9}Fe_2O_4$ nanostructures.

4. CONCLUSIONS

Doping of cobalt mixed oxide ($Ni_{0.1}Co_{0.9}Fe_2O_4$) with ZnO (0.46-2.25 wt%) followed by pre-calcination at 400-700°C effected an increase in its SBET (39-79%) and catalytic activity of hydrogen peroxide decomposition. The doping process resulted in a marked increase in the specific catalytic activity of ZnO-doped solids precalcined at 400-700°C. The mean size of crystallite of the pure and promoted ferrite particles calcined at 400°C are 45 nm and 27 nm respectively, which is well supported by the size obtained through SEM micrographs. The structural anode optical properties of the nanoparticles have been studied. The analysis of the data obtained from the optical experiments points to a direct allowed transition in the nanoparticles. The energy band gap in $Ni_{0.1}Co_{0.9}Fe_2O_4$ has been observed to be 5.0 eV.

REFERENCES

1. Cao D., Chao J., Sun L., Wang G., *Journal of Power Sources*, **179**(2008), 87.
2. Deraz N.A.M., *Materials Letters*, **57**(2002), 914.
3. Wang J., Deng T., Lin Y., Yang C., Zhan W., *Journal of Alloys and Compounds*, **450**(2008), 532.
4. Ji G.B., Tang S.L., Ren S.K., Zhang F.M., Gu B.X., Du Y.W., *Journal of Crystal Growth*, **270**(2004), 156.
5. Zhang G., Xu W., Li Z., Hu W., Wang Y., *Journal of Magnetism and Magnetic Materials*, **321**(2009), 1424.
6. Chaudhuri A., Mandal M., Mandal K., *Journal of Alloys and Compounds*, **487**(2009), 698.
7. Arshak K., Gaidan I., *Thin Solid Films*, **495**(2006), 286 .
8. Yardimci F.S., Senel M., Baykal A., *Materials Science and Engineering C*, **32**(2012), 269.
9. El-Shobaky G.A., Ghozza A.M., Deraz N.M., *Adsorp. Sci. Technol.*, **16**(1998), 21.
10. Sunclin S., Gurol A., *Environ. Sci. Technol.*, **32**(1998), 1417.
11. Hu Y.H., Ruckenstein E., *Catal. Lett.*, **36**(1996), 145.
12. Bartholomew C.H., *Catal. Lett.*, **7**(1990), 303.
13. Janardanarao M., *Ind. Eng. Chem. Res.*, **29**(1990), 1735.
14. Ruckenstein E., Hu Y.H., *J. Catal.*, **161**(1996), 55.
15. Ruckenstein E., Hu Y.H., *Appl. Catal.*, **133**(1995), 149.
16. Nichio N., Casella M., Ferretti O., Gonzalez M., Nicot C., Moraweck B., Frety R., *Catal. Lett.*, **42**(1996), 65.
17. Pal J., Chauhan P., *Materials characterization*, **61**(2010), 575.